ADVANCED MATERIALS

duced to 5 ppb, which is within the acceptable drinking water limits recommended by the US Environmental Protection Agency.

This work has demonstrated, using an example of environmental relevance, the vastly improved access of guest species to the binding sites of adsorbents designed from a mesostructure with well-defined mesopore channels, relative to those prepared from materials with disordered pore networks, such as silica gel. This accessibility principle is relevant to a broad range of materials applications where the availability of reactive sites is a performance-determining factor. Mesoporous molecular sieves thus constitute a unique class of oxides, from which a large number of nanoporous technologies could potentially be engineered based on the advantages of very high surface areas suitable for chemical functionalization and a uniform pore distribution for total access to the active sites.

Experimental

Starting material: HMS was prepared by the hydrolysis of TEOS in a dodecylamine solution following previously reported methods [7]. The product was then filtered and allowed to dry at room temperature overnight. The amine template was removed from the precipitated oxide by Soxhlet extraction over ethanol for 4 days.

Adsorbent preparation (MP-HMS): 1 g of HMS was dried under vacuum at 110 °C and refluxed with 1 g of 3-mercaptopropyltrimethoxysilane in 25 mL of dry toluene for 48 h. The functionalized product was then filtered, washed several times with toluene followed by ethanol, and subjected to Soxhlet extraction over ethanol for 18 h in order to remove residual (ungrafted) organosilane.

Characterization: Powder X-ray diffraction (XRD) patterns for HMS and MP-HMS were recorded on a Rigaku rotaflex diffractometer using Ni-filtered CuKα radiation. Proton-decoupled ^{29}Si MAS NMR spectra were recorded on a Varian VRX 400 MHz spectrometer at 79.5 MHz using 7 mm zirconia rotors, a sample spinning frequency of 4 kHz, and a pulse delay of 870 s. Nitrogen adsorption isotherms were measured at 77 K on a Coulter Omnisorp 360CX Sorptometer using standard continuous adsorption procedures. The samples were heated overnight at 110 °C and 10^{-6} torr prior to measurement. C, H, N, and S analyzes were performed by the Microanalysis Laboratory at the University of Illinois at Urbana-Champaign.

Hg adsorption studies: 10 mg portions of the functionalized mesostructure (MP-HMS) were stirred for 18 h with 50 mL volumes of mercury(II) nitrate solutions at initial concentrations ranging from 0 to 35 ppm. $Hg^{2\oplus}$ concentrations were determined before and after treatment by colorimetric analysis using diphenylthiocarbazone as an indicator [15]. Adsorption isotherms were generated by plotting the amount of Hg adsorbed per gram of MP-HMS as a function of the total (or initial) amount of $Hg^{2\oplus}$ per gram of adsorbent. For the packed-bed column experiment, part per billion levels of mercury were measured using cold-vapor atomic adsorption spectroscopy (DLZ Laboratories, Lansing, Michigan).

Received: December 12, 1996
Final version: February 3, 1997

[1] L. Mercier, C. Detellier, *Environ. Sci. Technol.* **1995**, *29*, 1318.
[2] M. S. Iamamoto, Y. Gushikem, *J. Colloid Interface Sci.* **1989**, *129*, 162.
[3] E. I. S. Andreotti, Y. Gushikem, *J. Colloid Interface Sci.* **1991**, *142*, 97.
[4] W. C. Moreira, Y. Gushikem, O. R. Nascimento, *J. Colloid Interface Sci.* **1992**, *150*, 115.
[5] R. M. Izatt, J. S. Bradshaw, R. L. Bruening, B. J. Tarbet, M. L. Bruening, *Pure Appl. Chem.* **1995**, *67*, 1069.
[6] J. S. Beck, J. C. Vartuli, W. J. Roth, M. E. Leonowicz, C. T. Kresge, K. D. Schmitt, C. T.-W. Chu, D. H. Olson, E. W. Sheppard, S. B. McCullen, J. B. Higgins, J. L. Schlenker, *J. Am. Chem. Soc.* **1992**, *114*, 10834.
[7] P. T. Tanev, T. J. Pinnavaia, *Science* **1995**, *267*, 865.
[8] S. A. Bagshaw, E. Prouzet, T. J. Pinnavaia, *Science* **1995**, *269*, 1242.
[9] T. M. Abdel-Fattah, T. J. Pinnavaia, *J. Chem. Soc., Chem. Commun.* **1996**, 665.
[10] E. Armengol, M. L. Cano, A. Corma, H. Garcia, M. T. Navarro, *J. Chem. Soc., Chem. Commun.* **1995**, 519.
[11] F. Schüth, *Ber. Bunsenges. Phys. Chem.* **1995**, *99*, 1306.
[12] T. Maschmeyer, F. Rey, G. Sankar, J. M. Thomas, *Nature* **1995**, *378*, 159.
[13] A. Cauvel, D. Brunel, F. DiRenzo, F. Fajula, *AIP Conf. Proc.* **1996**, *354*, 477.
[14] D. Brunel, A. Cauvel, F. Fajula, F. DiRenzo, *Stud. Surf. Sci. Catal.* **1995**, *97*, 173.
[15] Z. Marczenko, in *Spectrophotometric Determination of Elements* (Ed: C. G. Ramsay), Wiley, New York **1976**.

Superconducting RNi_2B_2C (R = Y, Lu) Nanoparticles: Size Effects and Weak Links**

By *Wolfgang K. Maser,* Patrick Bernier, Igor Luk'yanchuk, Philippe Molinié, Serge Lefrant, Philipp Redlich,* and *Pulickel M. Ajayan*

Nanoscale materials are the subject of extensive research.[1] They have a large potential for technological application in different fields, for example as active constituents of electronic circuits[2,3] and flat screen devices,[4] as ultrahigh density magnetic recording materials,[5] as reinforcing constituents in polymer composites,[6] and as constituents in high-temperature superconductors.[7] Furthermore, they are ideal materials to study the nature of finite size effects and dimensional crossover phenomena, for example in areas of magnetism[8] and superconductivity.[9]

The problem of building nanomaterials is tackled from several directions. More recently, the carbon arc-discharge technique[10] has promised to become a powerful route for the synthesis of carbon nanostructures[11,12] and simple metal (metal–carbon) nanophases.[8,13] Using this latter method, we report here the formation of superconducting nanoparticles belonging to the recently discovered intermetallic boron carbide family RNi_2B_2C (R = Y, Lu).[14,15] The parti-

[*] Dr. W. K. Maser, Dr. P. Bernier
Groupe de Dynamique des Phases Condensées
Université de Montpellier II
Place Eugène Bataillon
F-34095 Montpellier (France)
Dr. I. Luk'yanchuk[+]
L. D. Landau Institute for Theoretical Physics
2 Kosygina, 117940 Moscow (Russia)
Dr. P. Molinié, Prof. S. Lefrant
Institut des Materiaux de Nantes
Université de Nantes
2 rue de la Houssinière, F-44072 Nantes (France)
P. Redlich, Prof. P. M. Ajayan[++]
Max-Planck-Institut für Metallforschung
Institut für Werkstoffwissenschaft
Seestrasse 92, D-70174 Stuttgart (Germany)
[+] Present address: Universidade Federal de Minas Gerais, Departamento de Fisica, CP-702, 30.161-970 Bello Horizonte, MG, Brazil.
[++] Present address: Department of Materials Science and Engineering, Rensselaer Polytechnic Institute, Troy, NY 12180-3590, USA.

[**] This work was supported by the European Community through the TMR contract NAMITECH, ERBFMXC-CT96-0067 (DG12 – MIHT).

cles formed have diameters between 2 and 10 nm and are embedded in a glassy carbon matrix. We observe superconducting transitions at temperatures of T_c = 15 K for R = Y, and 16 K for R = Lu. The magnetic behavior is characterized by finite size effects and weak Josephson links between the nanocrystallites. With the formation of nanoparticles of this particular class of superconductors we show that the carbon arc is a valuable tool for the synthesis of complex and highly crystalline nanosize materials, including the growth of desired stoichiometries. It therefore offers the possibility to study the influence of particle size effects on the special properties of these materials.

Samples of stoichiometric superconducting RNi_2B_2C were prepared by electric arc discharge synthesis and collected in the form of a powderous material (see experimental section below for details). High resolution electron microscopy (HREM) showed the presence of spherical crystalline nanoparticles with diameters ranging from 2 to 10 nm (Fig. 1). These are found in a glassy carbon matrix

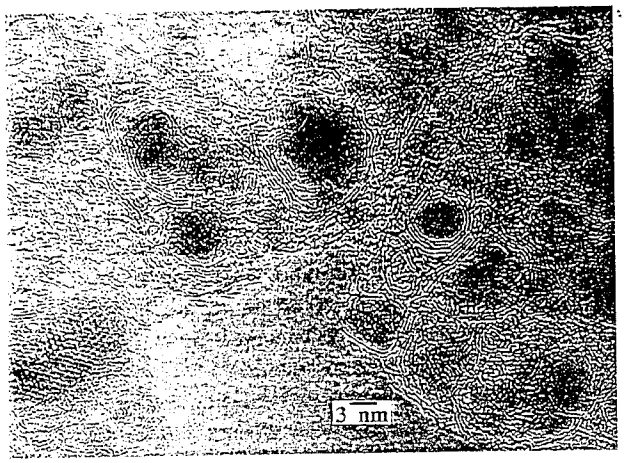

Fig. 1. HREM image from the Y–Ni–B–C sample showing spherical, highly crystalline particles embedded in a glassy carbon matrix. The diameter distribution ranges from 3 to 10 nm.

and constitute 25 % of the specimen area. The rest consisted of carbon nanotubes[11] and polyhedral carbon nanoclusters[12] (a few of the latter (about 5 %) were partially filled with highly crystalline material).

Electron energy loss (EELS) and energy dispersive spectroscopy (EDS) measurements (Figs. 2 and 3) revealed information about the composition of individual nanoparticles. Although it is difficult to unambiguously detect very low concentrations of Y by EELS (the yttrium M edge is delayed and overlaps partly with the boron K edge), in addition to the EDS detector limit, which does not extend to the detection of boron, the combination of the results of both techniques clearly reveals that the spherical particles contain all the elements used in the starting filling composition, indicating the formation of quaternary R–Ni–B–C intermetallic compounds. (In contrast to this, the crystalline fillings of the graphitic polyhedral clusters in both samples (R = Y, Lu) do not contain nickel—they are composed only

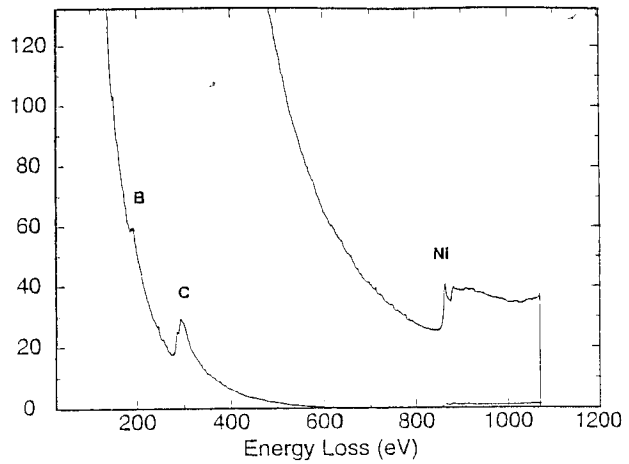

Fig. 2. Characteristic EELS spectrum of a spherical particle in the Y–Ni–B–C sample showing the K edges of boron and carbon and the L edge of nickel (shown with increased scaling for better presentation).

of non-superconducting R–B–C material.) However, the exact stoichiometry is seen to vary from particle to particle. In fact, the X-ray diffraction data of both samples point to highly crystalline multiphase material in which various R–Ni–B–C phases co-exist, and with the superconducting RNi_2B_2C material as a minor phase. It is hence understood that only a small percentage of the spherical particles contains the superconducting stoichiometry.

Figure 4 shows the temperature dependence of the magnetization between 4.5 and 25 K, measured under zero-field cooled (ZFC) and field cooled (FC) conditions in a field of 10 mT. The magnetization values were corrected for the normal state behavior between 16 and 40 K. The magnetic response clearly exhibits a transition into the superconducting state below T_c values of 15 and 16 K for R = Y and Lu, respectively. The transition is rather gradual and extends over a temperature range of a few kelvin. All the above observations point to the existence of superconducting nanocrystalline material of composition RNi_2B_2C in our samples (note that in the plethora of R–Ni–B–C bulk compounds, the superconducting phase is considered to be identical with the RNi_2B_2C phase).[14,16] The observed T_c values are ~0.6 K lower than in the corresponding bulk material. This effect can be explained by the small sizes of the nanoparticles in our samples. Since a vast majority of the particles have diameters below 10 nm, which corresponds to the superconducting coherence length ξ_o[16,17] of RNi_2B_2C, a shift to lower transition temperatures is introduced.[9] Additionally, the size distribution of these particles leads to the observed broad transition width in our samples.[9] Transition temperatures and transition widths were reproduced on samples prepared under the same experimental conditions as described below. The superconducting volume fractions estimated from the magnitude of the shielding signals correspond to 1–2 % (R = Y) and 0.1 % (R = Lu), showing again that the superconducting phase is only a minor phase in our samples.

0935-9648/97/0605-0504 $ 17.50+.50/0 Adv. Mater. 1997, 9, No. 6

ADVANCED MATERIALS

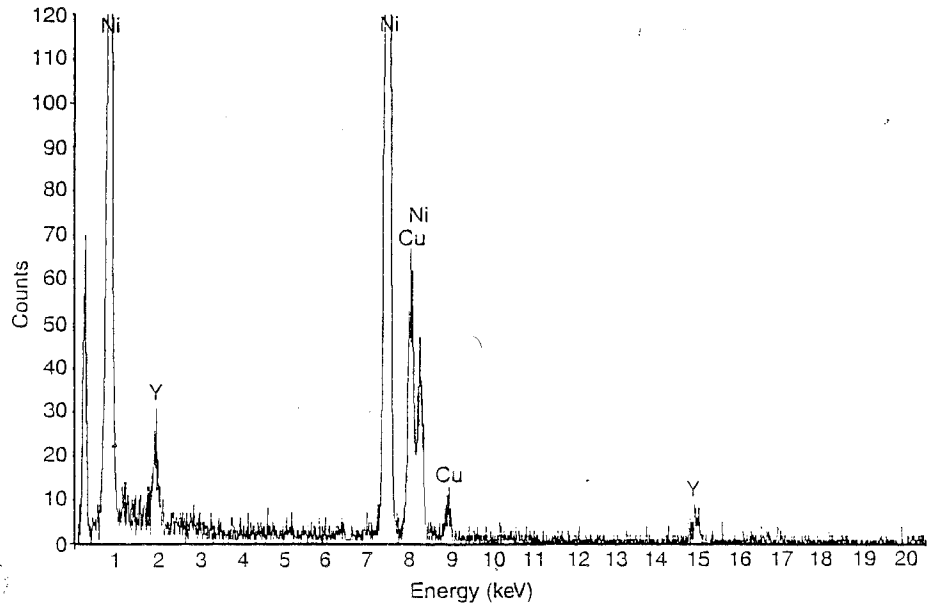

Fig. 3. EDS data from spherical particles in the Y–Ni–B–C sample reveal, typically, the presence of C (K_α), Ni (K_α, K_β, L_α, L_β) and Y (K_α, K_β, L_β). The observed Ni/Y ratio of individual particles can vary between 6 and 10. The Cu signals are due to the X-ray emission from the copper grid supporting the specimens.

In order to further characterize the superconducting nature we measured the temperature dependence of the magnetization ($M(T)$) under ZFC and FC conditions for the R = Y sample at several fields between 5 mT and 2 T. From the measurements we obtained at each field the value of the T_c-onset in the M_{FC} (T) curve, and in this way the temperature dependence of the upper critical field H_{c2}. In Figure 5, the $H_{c2}(T)$ curve is compared with the one for $H_{c2\,bulk}(T)$, the upper critical field of the YNi_2B_2C bulk material, which was obtained in the same manner.[18] The $H_{c2}(T)$ curve shows the same increasing characteristic with decreasing temperature as the $H_{c2\,bulk}(T)$ curve (there may be a deviation from the bulk behavior at temperatures above 14.5 K, but to further explore this, more data are needed). However, their values lie systematically below those of the bulk material. This behavior is possibly also related to the fact that the particle size is smaller than the coherence length ξ_0.

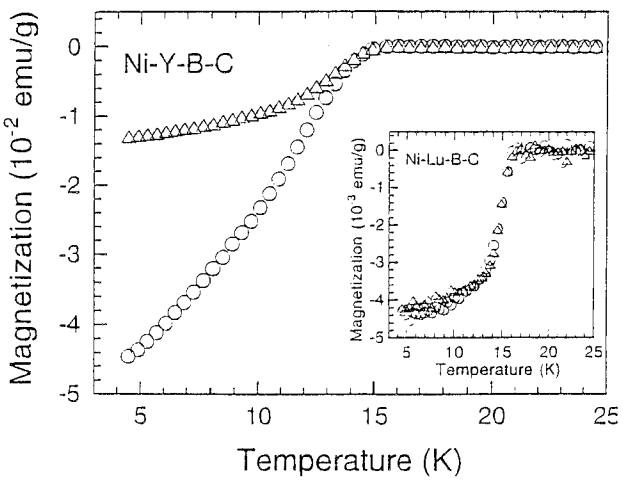

Fig. 4. Temperature dependence of the magnetization between 4 and 25 K at an applied field of 10 mT under zero field cooled △ and field cooled ○ conditions for both samples R = Y and Lu (inset).

As a next step, we extracted from our measurements the temperature dependence of the irreversible critical field $H_{irr}(T)$ by plotting at each field $\Delta M(T) = M_{FC}(T) - M_{ZFC}(T)$, and extrapolating to $\Delta M(T) = 0$. The results are presented in Figure 6 together with the corresponding curve for the bulk material, $H_{irr\,bulk}$.[18] In contrast with the bulk case, the irreversibility line $H_{irr}(T)$ is almost temperature independent and saturates at relatively small fields, indicating that the magnetization is reversible within a wide range of fields, first becoming irreversible below 0.5 T. The irreversibility effect cannot be explained by the Abrikosov vortex-pinning mechanism, as is the case for the bulk superconductor.[17] Since the size of the superconducting particles is smaller than the coherence length ξ_0, no trapped vortices can be formed and Meissner currents completely penetrate the particles. Therefore, the observed low-field hysteresis effects can be related to the appearance of weak Josephson links between the superconducting na-

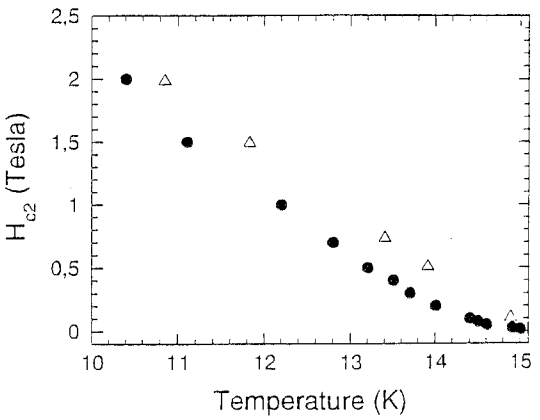

Fig. 5. Temperature dependence of the upper critical field H_{c2} for the R = Y sample ●. For comparison it is plotted together with the values of the upper critical field of the YNi_2B_2C bulk superconductor △, which are taken from [18].

  0935-9648/97/0605-0505 $ 17.50+.50/0

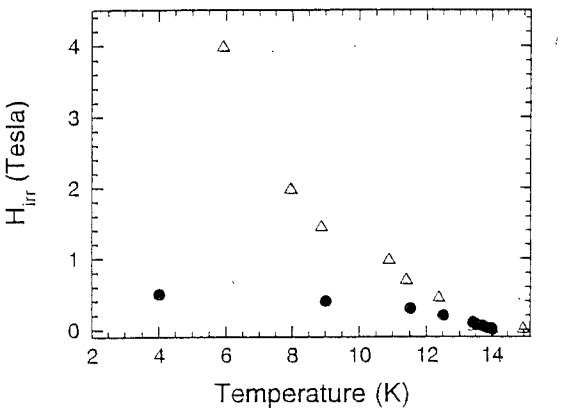

Fig. 6. Temperature dependence of the irreversible critical field H_{irr} for the R = Y sample ●. For comparison it is plotted together with the values of the irreversible critical field of the YNi_2B_2C bulk superconductor △, which are taken from [18].

nocrystallites, mediated by the carbon matrix. This Josephson junction array acts as an effective mechanism for magnetic flux pinning.[19] Assuming that H_{irr} is of the same order of magnitude as the field where the weak links appear, we estimate H_{irr} as $\Phi_0/2\pi\xi_j^2$, where Φ_0 is the magnetic flux quantum and ξ_j has the meaning of the coherence length of the Josephson junction array. From this, taking $H_{irr}(0) = 0.5$ T, we obtain a Josephson coherence length ξ_j of about 25 nm, corresponding to the characteristic cluster size of superconducting nanoparticles connected by the weak Josephson links.

To summarize, with the synthesis of superconducting RNi_2B_2C nanoparticles we establish the potential of the arc discharge technique for the growth of complex nanocrystalline systems. Several previous studies have shown that the technique is viable for the synthesis of nanophase systems but with simple binary compositions (metal-carbon systems). The possibility that we demonstrated here, that of forming quaternary compounds of useful stoichiometry, should pave the way for further scrutiny of the mechanisms of growth in the carbon arc, leading to better control of the process parameters and extension of this technique to other systems. This should allow the study of finite size effects in various complex materials.

Experimental

For the electric arc discharge synthesis we used a pure graphite cathode (16 mm in diameter), and a hollow graphite anode (6 mm in diameter with a 3.5 mm hole) filled with powders of the elements R, Ni, B, and C in the stoichiometric composition of RNi_2B_2C (the weight of the overall filling mixtures was 1000 mg. The mass of the individual constituents were for the YNi_2B_2C sample: Y: 374 mg, Ni: 486 mg, B: 90 mg, C: 50 mg, and for the $LuNi_2B_2C$ sample: Lu: 537.5 mg, Ni: 360.5 mg, B: 64.5 mg, C: 37.5 mg). The electric arc conditions were ~30 V and ~100 A at a reactor chamber pressure of 660 mbar of helium. After the arc-process, the filled part of the anode was consumed and a cylindrical deposit has grown on the cathode (length: 5 mm, diameter: 6 mm). About 50 mg of powdery material was collected from its inner core. Structural characterization of this inner core material was performed by HREM in a JEM 4000EX (JEOL) operating at 400 keV, by EELS, and EDS using a dedicated scanning transmission electron microscope (STEM) (VG HB501 UX operating at 100 keV), and by X-ray diffraction (INEL CPS120). For the HREM, EELS, and EDS measurements, one part of the sample was sonicated in ethanol and dispersed onto a copper grid with a holey carbon film. For all other measurements, the as-collected powdery material was used. The magnetic properties of the samples were investigated using a superconducting-quantum interference device (Quantum Design SQUID MPMS5).

Received: November 6, 1996
Final version: January 13, 1997

[1] J. Dutta, H. Hofmann, G. Schmid, *Adv. Mater.* **1996**, *8*, 555.
[2] J. Glan, *Science* **1995**, *269*, 1363.
[3] W. Ebbesen, *Annu. Rev. Mater. Sci.* **1994**, *24*, 235.
[4] W. de Heer, A. Châtelain, D. Ugarte, *Science* **1995**, *270*, 1179.
[5] T. Hayashi, S. Hirono, M. Tomita, S. Umemura, *Nature* **1996**, *381*, 772.
[6] P. M. Ajayan, O. Stephan, C. Colliex, D. Trauth, *Science* **1994**, *265*, 1212.
[7] P. Yang, C. Lieber, *Science* **1996**, *273*, 1836.
[8] M. E. McHenry, S. A. Majetich, J. O. Artman, M. DeGraef, S. W. Staley, *Phys. Rev. B* **1994**, *49*, 11 358.
[9] R. Goswami, S. Banerjee, K. Chattopadhyay, A. K. Raychaudhuri, *J. Appl. Phys.* **1993**, *73*, 2934.
[10] W. Krätschmer, L. D. Lamb, K. Fostiropoulos, D. R. Huffman, *Nature* **1990**, *347*, 354.
[11] S. Iijima, *Nature* **1991**, *354*, 57.
[12] Y. Saito, T. Yoshikawa, M. Inagaki, M. Tomita, T. Hayashi, *Chem. Phys. Lett.* **1993**, *204*, 277.
[13] R. S. Ruoff, D. C. Lorents, B. Chan, R. Malhotra, S. Subramoney, *Science* **1993**, *259*, 346.
[14] R. J. Cava, H. Takagi, H. W. Zandbergen, J. J. Krajewski, W. F. Peck Jr, T. Siegrist, B. Batlogg, R. B. van Dover, R. J. Felder, K. Mizuhashi, J. O. Lee, H. Eisaki, S. Uchida, *Nature* **1994**, *367*, 252.
[15] R. Nagarajan, C. Mazumdar, Z. Hossain, S. K. Dhar, K. V. Gopalakrishnan, L. C. Gupta, C. Godart, B. D. Padalia, R. Vijayaraghavan, *Phys. Rev. Lett.* **1994**, *72*, 274.
[16] N. M. Hong, H. Michor, M. Vybornov, T. Holubar, P. Hundegger, W. Perthold, G. Hilscher, *P. Rogl. Physica C* **1994**, *227*, 85.
[17] M. Xu, P. C. Canfield, J. E. Ostenson, D. K. Finnemore, B. K. Cho, Z. R. Wang, D. C. Johnston, *Physica C* **1994**, *227*, 321.
[18] S. B.Roy, Z. Hossain, A. K. Pradhan, C. Mazumdar, P. Chaddah, R. Nagarajan, C. Godart, L. C. Gupta, *Physica C* **1994**, *228*, 319.

0935-9648/97/0605-0506 $ 17.50+.50/0